

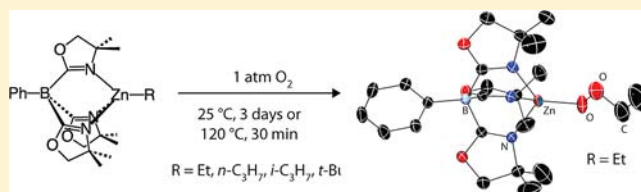
Remarkably Robust Monomeric Alkylperoxyzinc Compounds from Tris(oxazolinyl)boratozinc Alkyls and O₂

Debabrata Mukherjee, Arkady Ellern, and Aaron D. Sadow*

Department of Chemistry and United States Department of Energy Ames Laboratory, Iowa State University, Ames, Iowa 50011, United States

S Supporting Information

ABSTRACT: Metal alkylperoxides are remarkable, highly effective, yet often thermally unstable, oxidants that may react through a number of possible pathways including O–O homolytic cleavage, M–O homolytic cleavage, nucleophilic O-atom transfer, and electrophilic O-atom transfer. Here we describe a series of zinc alkyl compounds of the type To^MZnR (To^M = tris(4,4-dimethyl-2-oxazolinyl)phenylborate; R = Et, *n*-C₃H₇, *i*-C₃H₇, *t*-Bu) that react with O₂ at 25 °C to form isolable monomeric alkylperoxides To^MZnOOR in quantitative yield. The series of zinc alkylperoxides is crystallographically characterized, and the structures show systematic variations in the Zn–O–O angle and O–O distances. The observed rate law for the reaction of To^MZnEt (2) and O₂ is consistent with a radical chain mechanism, where the rate-limiting S_H2 step involves the interaction of •OOR and To^MZnR. In contrast, To^MZnH and To^MZnMe are unchanged even to 120 °C under 100 psi of O₂ and in the presence of active radical chains (e.g., •OOEt). This class of zinc alkylperoxides is unusually thermally robust, in that the compounds are unchanged after heating at 120 °C in solution for several days. Yet, these compounds are reactive as oxidants with phosphines. Additionally, an unusual alkylperoxy group transfer to organosilanes affords To^MZnH and ROOSiR₃'.



1. INTRODUCTION

Reactions of alkylzinc reagents and O₂ provide environmentally and economically appealing approaches for useful oxidations, including epoxidations,¹ hydroxylations,² and peroxidations.³ In addition, alkylzinc compounds and their reactions with oxygen are fundamentally interesting because zinc occupies a unique position as a nontransition-element and nonredox active divalent metal center whose chemistry nonetheless bears resemblance to the 3d metals. Reactions of (nonmetallic) alkylboranes and O₂ provide a close well-studied main-group system and are proposed to follow a radical chain based on compelling evidence from kinetic studies, inhibition by radical traps such as galvinoxyl, stereochemical studies, and spectroscopic radical trapping experiments. Galvinoxyl similarly inhibits the reactions of ZnR₂ and O₂,⁴ and additional evidence for open-shell alkyl, alkoxy, and alkylperoxy intermediates is provided by EPR spectroscopy of trapped species.⁵ Oxygen initiates carbocationizations, which is taken as evidence for a radical chain pathway.^{6,7} However, direct kinetic support for a radical chain reaction is limited,⁴ and a rate law for the reaction of alkylzinc compounds and O₂ has not even been reported.

Furthermore, detailed mechanistic investigations of reactions between organotransition-metal compounds and O₂ have provided a number of mechanisms, including the radical chain, O₂ coordination/protonation, and direct insertion.⁸ Likewise, several pathways have been proposed for oxidations and metal alkylperoxide formations involving main-group organometallic systems including zinc.^{4,5,9} At one extreme, •R or •OOR, formed through a radical chain, could directly oxidize

an organic substrate. A radical chain could also give discrete [Zn]OOR intermediates, or alternatively such alkylperoxyzinc species could form via electron-transfer steps that exclude the chain reaction. Low-temperature reactions of L₂ZnR₂ (L = 4-methylpyridine, 1,4-diazabutadiene, 2,2'-(1'-pyrrolinyl)pyrrole) and O₂ that yield isolable and crystallographically characterized alkylperoxyzinc species provide support for the latter mechanism.^{9c,10,11} However, the products of these reactions invariably contain multimetallic bridging alkoxides and/or alkylperoxides that can obscure the reaction mechanism.

Highly reactive, alkylperoxy main-group compounds [M]OOR (M = Mg,¹² Zn,^{9c,10,13} Ga,¹⁴ In)¹⁵ have been prepared from organometallics and O₂, although these systems are not amenable to quantitative kinetic investigations. For example, Parkin's seminal Tp^{*t*-Bu}MgOOR compounds (Tp^{*t*-Bu} = HB(N₂C₃H₂*t*-Bu)₃; R = Me, Et, *i*-C₃H₇, *t*-Bu) are proposed to form through a radical chain pathway based on galvinoxyl inhibition, and the relative rates follow the expected stability of •R.¹² Interestingly, the analogous Tp^{*t*-Bu}ZnR compounds and O₂ do not provide detectable quantities of Tp^{*t*-Bu}ZnOOR.¹⁶ The diketiminate ligand supports a monomeric aluminum *tert*-butylperoxide formed from alkane elimination with HOO*t*-Bu,¹⁷ but bridging alkylperoxy-magnesium and zinc species are formed from (diketiminate)MR and O₂ [M = Mg, R = CH₂Ph;^{12c} M = Zn, R = Et].¹³ Monomeric structures may have enhanced kinetic stability because [M]R and [M]OOR can

Received: April 10, 2012

Published: July 30, 2012

comproportionate through multimetallic structures to metal alkoxides.² Still, monomeric, divalent, tetrahedral 3d transition-metal alkylperoxides, stabilized by bulky tris(pyrazolyl)borate ligands, decompose rapidly by homolysis at room temperature.¹⁸

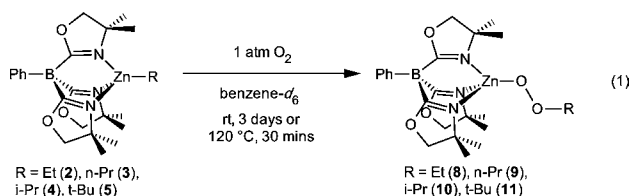
Kinetic investigations of reactions of $[Zn]R$ and O_2 , then, may be simplified by monomeric alkylperoxyzinc products. The tridentate monoanionic tris(4,4-dimethyl-2-oxazolanyl)-phenylborate ligand $[To^M]$ supports monomeric zinc hydride, alkyls, amides, and alkoxides,¹⁹ and therefore this ancillary ligand might also stabilize zinc alkylperoxides. Here, we report the synthesis and characterization of a series of remarkably robust, monomeric, terminal To^MZnOOR compounds and kinetic studies of their formation from reactions of O_2 and To^MZnR as well as their slow decomposition and mild atom- and group-transfer reactivity.

2. RESULTS AND DISCUSSION

2.1. Synthesis and Characterization of To^MZnOOR ($R = Et, n-C_3H_7, i-C_3H_7, t-Bu, CMe_2Ph$). A series of zinc alkyl compounds To^MZnR [$R = Me$ (1),^{19b} Et (2), $n-C_3H_7$ (3), $i-C_3H_7$ (4), $t-Bu$ (5), Ph (6), CH_2Ph (Bn; 7)] is synthesized by metathesis from $Tl[To^M]$ and ZnR_2 , protonolysis of ZnR_2 with HTo^M , or salt elimination of To^MZnCl and RLi .²⁰ Some of these compounds are precursors to the targeted To^MZnOOR species. Compounds 1–7 are characterized by spectroscopic and analytical methods as well as single crystal diffraction for all compounds except 4. Compounds 1–7 are all pseudo- C_{3v} symmetric, as indicated by equivalent oxazoline groups in 1H and ^{13}C NMR spectra. This spectroscopy is consistent with tridentate coordination of the tris(oxazolanyl)borate ligand to a single zinc center. Additionally, the 1H NMR spectra contained diagnostic upfield resonances assigned to the $\alpha-CH$ of the $Zn-R$ moiety. These spectral data are consistent with the monomeric structures and four-coordinate zinc centers confirmed by single crystal X-ray diffraction studies (see Figure 1 for 2 and Figures S-13–16 in the Supporting Information (SI) for 3 and 5–7).

Compounds 1–7 are resistant to thermal decomposition; for example, compound 2 was recovered quantitatively after thermolysis at 170 °C for 24 h in a sealed NMR tube. Thus, initiation of the radical chain mechanism, proposed for reactions with O_2 (vide infra), is unlikely to involve spontaneous $Zn-C$ bond homolysis in this system.^{10a}

Compounds 2–5 react with O_2 (1 atm) in benzene- d_6 over 3 days at room temperature, 6–8 h at 60 °C, or 30 min at 120 °C to form To^MZnOOR [$R = Et$ (8), $n-C_3H_7$ (9), $i-C_3H_7$ (10), $t-Bu$ (11)] as the only species detected (eq 1). These synthetic



conditions highlight the remarkable thermal stability of 8–11 and strongly contrast the low-temperature preparation and kinetic lability typically associated with 3d transition-metal and many main-group alkylperoxides.

Compounds 8–11 form quantitatively, and evaporation of the reaction mixtures provides analytically pure products. The

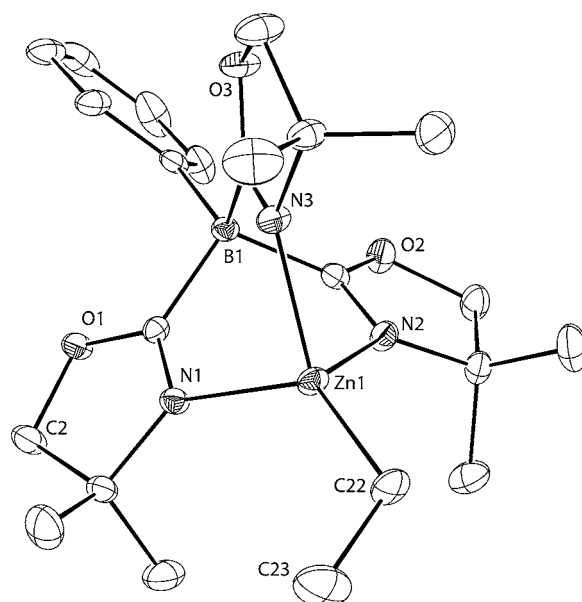


Figure 1. ORTEP diagram of To^MZnEt (2). Significant interatomic distances (Å): $Zn1-C22$, 1.994(2); $Zn1-N1$, 2.058(1); $Zn1-N2$, 2.084(1); $Zn1-N3$, 2.075(1). Significant interatomic angles (°): $Zn1-C22-C23$, 118.7(1); $N1-Zn1-C22$, 128.83(6); $N2-Zn1-C22$, 120.53(7); $N3-Zn1-C22$, 126.35(7).

room temperature 1H NMR spectra of 8–11 contain resonances assigned to equivalent oxazoline groups that suggest pseudo- C_{3v} symmetry for the To^M ligand. Downfield $[Zn]-OCH$ resonances of 8–10 replace the upfield $[Zn]CH$ signals of 2–4. However, *tert*-butyl 5 and *tert*-butylperoxy 11 are distinguished only by the $^{13}C\{^1H\}$ NMR resonance for the CMe_3 that shifts from 35.82 to 77.60 ppm.

^{17}O NMR spectra are obtained from samples of ^{17}O -enriched 8–11 that are synthesized by treatment of compounds 2–5 with $^{17}O_2$ in benzene- d_6 . The data are listed in Table 1. Interestingly,

Table 1. ^{17}O NMR Chemical Shifts of To^MZnOOR and $Tp^{t-Bu}MgOOR$ (vs H_2O)

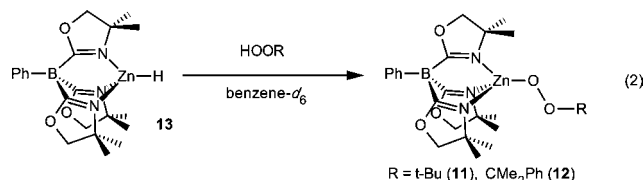
	$\delta([M]OOR)$	$\delta([M]OOR)$
$To^MZnOOEt$ (8)	319	169
$Tp^{t-Bu}MgOO(Et)^a$	407	130
$To^MZnOO(n-Pr)$ (9)	322	167
$To^MZnOO(i-Pr)$ (10)	304	193
$Tp^{t-Bu}MgOO(i-Pr)^a$	373	159
$To^MZnOO(t-Bu)$ (11)	284	204
$Tp^{t-Bu}MgOO(t-Bu)^a$	323	183

^aData from ref 12b.

the chemical shifts for the two resonances in 8- $^{17}O_2$ are similar to the shifts for 9- $^{17}O_2$. The chemical shift differences for the two resonances from 10 ($\Delta(\delta O) = \delta O_\alpha - \delta O_\beta = 111$ ppm) are smaller than the differences in 8 and 9 ($\Delta(\delta O) = 150$ and 155 ppm, respectively). The *tert*-butyl compound 11 gives even smaller differences in ^{17}O NMR chemical shifts ($\Delta(\delta O) = 80$ ppm). A similar observation was reported for $Tp^{t-Bu}MgOOR$ compounds, and by comparison we assign the downfield signal as $[Zn]OOR$, whereas the upfield resonance is attributed to $[Zn]OOR$. Interestingly, the $ZnOOR$ signals are upfield relative to the chemical shifts of $Tp^{t-Bu}MgOOR$, and the $[Zn]OOR$ is

downfield with respect to the corresponding magnesium alkylperoxide.

Additionally, compounds **11** and $\text{To}^M\text{ZnOOCMe}_2\text{Ph}$ (**12**) are readily prepared by reaction of To^MZnH (**13**) with HOOt-Bu and HOOCMe_2Ph , respectively (eq 2).



As noted in the Introduction, the related $\text{Tp}^{t\text{-Bu}}\text{ZnEt}$ is not oxidized by O_2 even at $100\text{ }^\circ\text{C}$.²¹ Surprisingly, only starting materials are evident after treatment of To^MZnMe (**1**) and To^MZnH (**13**) with O_2 from room temperature to $120\text{ }^\circ\text{C}$ and from 1 atm to 100 psi for 12 h. Addition of O_2 to mixtures of **2** and **1** or **13** converts **2** to **8**, while **1** or **13** remains unreacted. Alternatively, To^MZnPh (**6**) and To^MZnBn (**7**) react under O_2 at $120\text{ }^\circ\text{C}$ to form $(\kappa^2\text{-To}^M)_2\text{Zn}$ (**14**) in benzene over 48 h (see Figure S-22, SI). Compound **14** is prepared independently from $\text{Ti}[\text{To}^M]$ and **13**. Neither light nor the radical initiator AIBN facilitates reactions of **1**, **6**, **7**, and **13** with O_2 to provide isolable organoperoxy zinc species.

Reactions of oxygen and alkylzinc compounds are known to often yield alkoxides rather than peroxides, and the synthesis of alkylperoxy zinc compounds typically requires carefully controlled conditions to avoid formation of alkoxides.^{3,9,10} To^MZnOR is not formed in these reactions based on the combustion analyses of **8–12**, the X-ray structures (see below), the poorer benzene solubility of To^MZnOR (R = Et, *n*- C_3H_7 , *i*- C_3H_7) in comparison to **8–10**, and the nonequivalence of the ^1H NMR spectra of **8–11** to spectra obtained from treatment of To^MZnH with ROH (R = Et, *n*- C_3H_7 , *i*- C_3H_7 , *t*-Bu). Interestingly, these reactions of alcohols give broad ^1H NMR resonances in benzene; upon evaporation of volatile materials, benzene-insoluble white solids are obtained that suggest oligomeric structures. (The bulkier $\text{To}^M\text{ZnOt-Bu}$ is monomeric and soluble in benzene, and it is also spectroscopically distinct from **11**.)^{19a} The monomeric structures of **8–12** are verified by X-ray crystallography (see Figure 2 for **8** and Figures S-18–21, SI, for **9–12**). The alkylperoxy group of **9** is disordered over two positions and will not be discussed.

The Zn-O_α distances in **8** and **10–12** are similar (from $1.873(2)\text{ \AA}$ in **10** to $1.877(1)\text{ \AA}$ in **8**). Bridging [diketiminato $\text{Zn}(\mu^2\text{-OOEt})_2$] contains longer Zn–O distances [$1.971(1)$ and $2.044(1)\text{ \AA}$],¹³ and triply bridging $\text{Zn}_3(\mu^3\text{-OOME})$ Zn–O distances are much longer (2.132 \AA average) in the tetrameric cube $[(\text{MeZn})_4(\mu^3\text{-OOME})_2(\mu^3\text{-OZnMeL})_2]$ (L = diazabutadiene).¹⁰ However, the related alkoxide $\text{To}^M\text{ZnOt-Bu}$ contains a shorter Zn–O distance of $1.835(1)\text{ \AA}$.^{19a} Additionally, the general structural features of **8–12** are roughly similar to those of crystallographically characterized monomeric tris(pyrazolyl)borato transition-metal alkylperoxides.¹⁸ These 3d transition-metal alkylperoxides are typically synthesized from hydroperoxides which limits the diversity of readily accessible alkyl groups. The preparation of **8–11** from O_2 , as well as the availability of cumylperoxy **12**, provides a range of alkylperoxy zinc compounds for structural comparison.

Interestingly, the compound with the longest O–O distance contains the smallest Zn–O–O angle and shortest Zn– O_β distance (Table 2). Thus, the O–O distances follow the trend

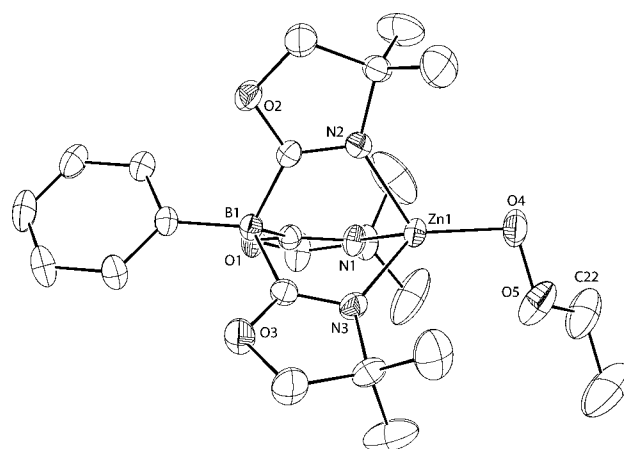


Figure 2. ORTEP diagram of To^MZnOOEt (**8**); ellipsoids are plotted at 35% probability, and hydrogen atoms and a toluene solvent molecule are not plotted. Significant interatomic distances (\AA): Zn1–O4, $1.877(1)$; Zn1–O5, $2.630(2)$; Zn1–N1, $2.027(1)$; Zn1–N2, $2.045(1)$; Zn1–N3, $2.033(1)$; O4–O5, $1.466(2)$. Significant interatomic angles ($^\circ$): Zn1–O4–O5, $103.1(1)$; N1–Zn1–O4, $121.34(6)$; N2–Zn1–O4, $119.87(6)$; N3–Zn1–O4, $128.53(6)$.

Table 2. Comparison of Interatomic O–O and Zn–O (\AA) Distances and Zn–O–O Angles ($^\circ$) for Compounds **8** and **10–12**

compound	O–O	$\angle\text{Zn–O–O}$	Zn– O_β
To^MZnOOEt (8)	$1.466(2)$	$103.1(1)$	$2.630(2)$
$\text{To}^M\text{ZnOO}(i\text{-C}_3\text{H}_7)$ (10)	$1.441(3)$	$105.1(1)$	$2.644(2)$
$\text{To}^M\text{ZnOOt-Bu}$ (11)	$1.490(2)$	$97.11(9)$	$2.534(2)$
$\text{To}^M\text{ZnOOCMe}_2\text{Ph}$ (12)	$1.477(3)$	$103.4(2)$	$2.637(2)$

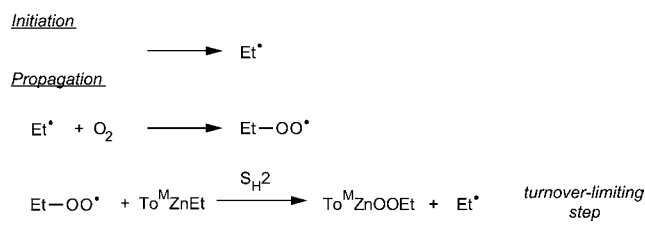
$10 < \mathbf{8} < \mathbf{12} < \mathbf{11}$ that inversely tracks the Zn– O_α – O_β angles and the Zn– O_β distances $\mathbf{11} < \mathbf{8} \sim \mathbf{12} < \mathbf{10}$. All of the Zn– O_β distances in **8** and **10–12** are within the sum of Zn and O van der Waals radii (2.91 \AA) but well outside the sum of covalent radii for Zn and oxygen (1.88 \AA).²² The nature of that interaction may be considered in the context of the systematically monomeric structures for **8–12** that contrast dimeric or oligomeric $[\text{To}^M\text{ZnOR}]_n$ (R = Et, *n*- C_3H_7 , *i*- C_3H_7) compounds. As noted above, the spectroscopic and physical properties of To^MZnOR are more consistent with oligomeric structures. Thus, the Zn– O_β interaction likely perturbs the atomic distances to a small but important degree to stabilize compounds **8–12** as the first structurally characterized monomeric zinc alkylperoxides.

2.2. Mechanistic Investigations and Kinetics of To^MZnR and O_2 . General observations for the reactions of To^MZnR and O_2 allow comparison to alkylzinc/ O_2 systems that are less amenable to rate law determinations. Reactions of To^MZnEt (**2**) and O_2 (50 psi) performed under ambient lighting and in the dark give equivalent conversion of **2** and yield (93%) of **8** after 32 h. Galvinoxyl inhibits the conversion. The To^MZnOOR compounds are the only detectable products from reactions of **2**, **3**, **4**, or **5** with O_2 in the presence or absence of azobis(isobutyronitrile) (AIBN). Species, such as C_4H_{10} , C_2H_6 , $\text{To}^M\text{ZnCMe}_2\text{CN}$, $\text{To}^M\text{ZnOOCMe}_2\text{CN}$ (or related products from **3–5**), that might be expected from radical initiation or termination processes are not observed for reactions of oxygen and To^MZnEt .

Rate law measurements for the reaction of **2** and O_2 from $45\text{--}96\text{ }^\circ\text{C}$ and $30\text{--}100\text{ psi}$ O_2 were thwarted by variable

induction periods and inconsistent concentration dependencies for both O_2 and $To^M ZnEt$. However, in the presence of AIBN (0.2–1.3 equiv), plots of $[2]$ vs time follow an exponential decay providing the pseudofirst-order rate constant k_{obs} . Notably, k_{obs} values are equivalent within error at O_2 pressures of 30, 50, 70, 80, and 100 psi, showing zero-order oxygen dependence (Figure S-3, SI). A linear correlation of $[AIBN]^{1/2}$ vs k_{obs} passes through the origin ($[2]_{ini} = 25$ mM, $[AIBN]_{ini} = 5.4$ – 33.9 mM, 54 °C), giving the rate law $-d[2]/dt = k'[2]^1[O_2]^0[AIBN]^{1/2}$ ($k' = 3.0 \pm 0.1 \times 10^{-3} M^{-1/2} s^{-1}$) which appears valid over at least three half-lives of the reaction time course. This rate law is consistent with a radical chain mechanism (Scheme 1) and is similar to empirical rate laws

Scheme 1. Proposed Radical Chain Mechanism for $To^M ZnOOEt$ Formation from $To^M ZnEt$ and O_2



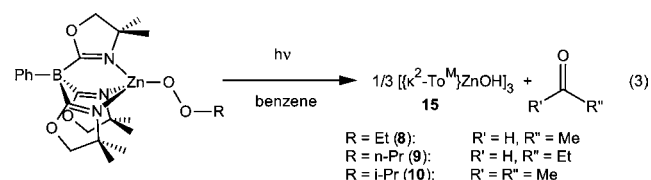
for autoxidation of organic compounds, organoboranes,² and a few O_2 insertions into transition-metal alkyls. Thus, our studies provide the first rate law-based support for a radical chain process for the interaction of alkylzinc species and O_2 .

The postulated radical chain mechanism includes a bimolecular homolytic substitution process (S_H2) at zinc that likely involves an electron transfer from the HOMO (the Zn–C bond) to *OOEt to form a Zn–O bond and *Et . The inert nature of $To^M ZnMe$ (1) and $To^M ZnH$ (13) with O_2 under these conditions suggests that *OOR ($R = H, Me$) is not able to oxidize the Zn–H and Zn–Me bonds even in the presence of AIBN and initiated radical chains (i.e., *OOEt).

Previously, the weaker $EtZn$ – Et bond vs $MeZn$ – Me provided a rationalization for the slower reaction of oxygen and $ZnMe_2$ in comparison to $ZnEt_2$.⁵ Although the bond dissociation energies (BDE's) for $To^M Zn$ – R have not yet been determined, the values are expected to follow the trends of RZn – R , which have been determined from statistical unimolecular reaction calculations (RRKM theory): $EtZn$ – $Et < MeZn$ – Me ($EtZn$ – $CH_2CH_3 = 219 \pm 8$ kJ/mol (52.4 ± 2.0 kcal/mol); $MeZn$ – $CH_3 = 266.5 \pm 6.3$ kJ/mol (63.7 ± 1.5 kcal/mol)).²³ However, the experimental intrinsic BDE (determined from the ion beam method) for $[Zn-H]^+$ is much smaller than $[Zn-CH_3]^+$ BDE: $[Zn-H]^+ = 231 \pm 13$ kJ/mol (55.2 ± 3.1 kcal/mol); $[Zn-CH_3]^+ = 295 \pm 13$ kJ/mol (70.6 ± 3.2 kcal/mol).²⁴ The intrinsic BDE's also provide the BDE for $MeZn$ – CH_3 as 290 ± 13 kJ/mol (69.3 ± 3.2 kcal/mol) for comparison between the two sets of values. Regardless, the inert nature of $To^M ZnH$ toward O_2 is not readily rationalized by known BDE's.

2.3. Oxidation Reactivity of $To^M ZnOOR$. The concentration of $To^M ZnOOEt$ in benzene- d_6 is unchanged after 24 h at 120 °C in a sealed NMR tube. After 3 days at 140 °C, 63% of $To^M ZnOOEt$ is converted to $(\kappa^2-To^M)_2Zn$ (14). *Tert*-butylperoxide 11 is even slower to form 14 (30% after 3 d at 135 °C), and cumylperoxy 12 is unchanged after 1 d at 165 °C. Photolysis of the alkylperoxy zinc compounds 8–12 (350 nm, benzene, room temperature) provides a trimeric zinc hydroxide

species $[(\kappa^2-To^M)_2Zn(\mu-OH)]_3$ (15) that deposits as white crystals over 24 h (eq 3). The organic carbonyl products are



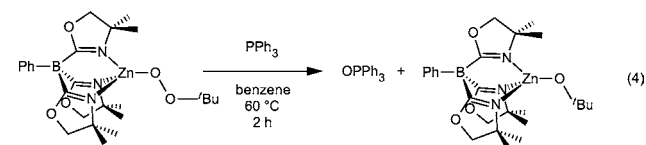
$MeCHO$, Me_2CO , and $EtCHO$ from 8, 9, and 10, respectively. Compound 11 forms Me_2CO , while the cumylperoxyzinc 12 forms acetophenone, methane, and the epoxide 2-methyl-2-phenyloxirane.

X-ray crystallography of disordered 15 establishes its connectivity as a trimeric $[Zn(\mu-OH)]_3$ structure. Compound 15 is soluble in methylene chloride but insoluble in benzene, toluene, and tetrahydrofuran. The room temperature 1H NMR spectrum of 15 in methylene chloride- d_2 was broad. The spectrum resolved at -53 °C indicated local C_s symmetry with equivalent zinc centers that are related by a rotation axis that is assumed to be C_3 based on the solid-state structure. Bidentate coordination of To^M to Zn in 15 is further supported by two oxazoline ν_{CN} bands in the IR spectrum at 1577 (coordinated) and 1623 cm^{-1} (noncoordinated) in an approximately 2:1 ratio.

The formation of zinc hydroxide and an oxidized organic species is consistent with O–O homolysis; for example, thermal decomposition of $Cp^*_2Hf(Ph)OOR$ gives $Cp^*_2Hf(Ph)OH$,²⁵ and photolysis of dialkylperoxides is well-known to provide two *OR that decompose to similar products.²⁶ Compound 15 is a likely intermediate in the thermolysis of alkylperoxides 8–12. That process also likely involves homolytic O–O bond cleavage because thermal treatment of 15 (in benzene- d_6) gives 14 (8 h, 120 °C). Conversion of 15 to 14 is faster than the overall rate of alkylperoxide decomposition, making that step kinetically competent for the overall conversion. Thus, the rate-determining step of conversion of 8–12 to 14 is O–O bond homolysis.

The thermal stability of the $[Zn]OOR$ moieties is remarkable in comparison to related main-group and transition-metal species, and this may be at least partly related to the monomeric nature of compounds 8–12. We therefore further investigated their reactivity for comparison with zinc alkylperoxides known to have multimetallic or unknown structures. For example, rapid comproportionation of alkylzinc and alkylperoxyzinc compounds to alkoxyzinc species starkly contrasts the present system. 1H NMR spectra of mixtures of alkylperoxyzincs 8–11 with the corresponding tris(oxazolonyl)boratozinc alkyl (2, 3, 4, or 5) or hydride 13 only contained signals assigned to starting materials, even after the mixtures were heated at 80 °C for 12 h.

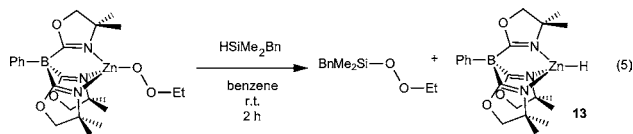
Despite their thermal stability, 8–12 are reactive in oxidation processes and group transfer chemistry. Compounds 8–12 readily react with phosphines, such as PH_2Ph , PPh_3 , $P(p-C_6H_4Me)_3$, and PMe_3 , to form the corresponding phosphine oxides via stoichiometric O-atom transfer (eq 4). Kinetic



studies of stoichiometric phosphine oxidations, particularly on a series of isolable monomeric alkylperoxymetal compounds, are surprisingly rare even though a range of mechanisms are conceivable (and proposed in related metal-alkylperoxide systems), including radical chains via O–O bond homolysis to give alkoxyradical intermediates,²⁷ nucleophilic attack of the phosphine on an η^2 -peroxyzinc, and coordination of phosphine to zinc followed by nucleophilic attack by the alkylperoxide.^{28,29}

Reaction rates for To^MZnOOR -*t*-Bu and PR_3 follow the trend $\text{PPh}_3 < \text{P}(p\text{-C}_6\text{H}_4\text{Me})_3 < \text{PMe}_3 < \text{PH}_2\text{Ph}$; PPh_3 reacts in less than 2 h at 60 °C, whereas PMe_3 reacts in less than 5 min at ambient temperature. The second-order rate law $-\text{d}[\text{To}^M\text{ZnOOR}]/\text{d}t = k[\text{To}^M\text{ZnOOR}][\text{P}(p\text{-C}_6\text{H}_4\text{Me})_3]$ emphasizes the mononuclear nature of alkylperoxyzinc species and the bimolecular nature of the reaction. The rate constants follow the trend: $8 > 9 > 10 \gg 11$ ($k_{259\text{K}}^{(8)} = 8.8 \pm 0.3 \times 10^{-2}$, $k_{259\text{K}}^{(9)} = 7.5 \pm 0.2 \times 10^{-2}$, $k_{259\text{K}}^{(10)} = 6.3 \pm 0.2 \times 10^{-3}$, $k_{294\text{K}}^{(11)} = 1.22 \pm 0.04 \times 10^{-3} \text{ M}^{-1}\text{s}^{-1}$; $[\text{P}(p\text{-C}_6\text{H}_4\text{Me})_3] = 30 \text{ mM}$) showing steric effects in the reactivity of the alkylperoxyzinc reagents. Eyring analysis of the reaction between **8** and $\text{P}(p\text{-C}_6\text{H}_4\text{Me})_3$ provides $\Delta H^\ddagger = 9.5 \pm 0.3 \text{ kcal}\cdot\text{mol}^{-1}$ and $\Delta S^\ddagger = -27 \pm 1 \text{ cal}\cdot\text{mol}^{-1}\cdot\text{K}^{-1}$.³⁰ The second-order rate law, activation parameters, and reaction conditions rule out a unimolecular mechanism for phosphine oxidation by To^MZnOOR involving oxygen–oxygen bond homolysis.²⁷ The rate of $\text{P}(p\text{-C}_6\text{H}_4\text{Me})_3$ oxidation by **8**–**11** follows the size of the peroxyalkyl group (*t*-Bu < *i*-C₃H₇ < *n*-C₃H₇ < Et), but no relationship with Zn–O–O angles or O–O distances (obtained from the X-ray data) could be identified. Faster reaction rates with smaller alkyl groups suggest the mechanism involving nucleophilic attack of phosphine on an electrophilic alkylperoxide.

2.4. Alkylperoxy Group Transfer Reactivity with Hydrosilanes. In addition to the phosphine oxidation via O-atom transfer, metal peroxides are also known to oxidize C–H and Si–H bonds to give alcohol and silanol (SiOH) groups, respectively.^{19b,29,31} In contrast, the To^MZnOOR compounds **8**–**12** react with organosilanes (HSiR'_3) by peroxy-group transfer to silicon. For example, **8** and HSiMe_2Bn react according to eq 5. This alkylperoxy-group transfer reactivity



resembles previously observed alkoxy-group transfer to silicon from zinc alkoxides,^{19b} and that reaction is likely important in zinc-catalyzed dehydrocoupling of alcohols and silanes as well as hydrosilylation of carbonyls.³² Related Si–O bond formations may be involved in transition-metal, rare earth, and main-group metal catalyzed hydrosilylations.³³ While zinc alkylperoxides may be hydrolyzed to alkyl hydroperoxides,^{3,34} the hydrolysis product is $[\text{Zn}]\text{OH}$. In the reactions here with organosilanes, To^MZnH is the product, and that gives a possibility for (future) catalysis (e.g., zinc-catalyzed hydrosilylation of O_2).

The empirical rate law for the reaction of **8** and BnMe_2SiH of $-\text{d}[\text{To}^M\text{ZnOOR}]/\text{d}t = k[\text{To}^M\text{ZnOOR}][\text{BnMe}_2\text{SiH}]$ ($k_{309\text{K}} = 1.64 \pm 0.09 \times 10^{-2} \text{ M}^{-1}\text{s}^{-1}$) was measured from 288 to 320 K. The steric effects in this reactivity of the zinc alkyl peroxides also follow a similar trend as observed in phosphine oxidation: $8 > 9 > 10$ ($k_{309\text{K}}^{(8)} = 1.64 \pm 0.09 \times 10^{-2}$, $k_{309\text{K}}^{(9)} = 1.17 \pm 0.02 \times 10^{-2}$, $k_{309\text{K}}^{(10)} = 1.9 \pm 0.02 \times 10^{-3} \text{ M}^{-1}\text{s}^{-1}$). The activation

parameters for the reaction of **8** and BnMe_2SiH , $\Delta H^\ddagger = 12.6 \pm 0.7 \text{ kcal}\cdot\text{mol}^{-1}$ and $\Delta S^\ddagger = -26 \pm 2 \text{ cal}\cdot\text{mol}^{-1}\cdot\text{K}^{-1}$, are consistent with an ordered transition state associated with a second-order process.³⁰ Primary isotope effects for the reactions of To^MZnOOR and BnMe_2SiH or BnMe_2SiD are unity [$k_{\text{H}}/k_{\text{D}}^{(8)} = 1.10(7)$, $k_{\text{H}}/k_{\text{D}}^{(10)} = 1.11(9)$].

For comparison, the second-order Si–O bond forming reaction of the aryloxyzinc $\text{To}^M\text{ZnOC}_6\text{H}_3\text{Me}_2$ and PhMeSiH_2 occurs with similar activation parameter values ($\Delta H^\ddagger = 13 \text{ kcal}\cdot\text{mol}^{-1}$; $\Delta S^\ddagger = -27 \text{ cal}\cdot\text{mol}^{-1}\cdot\text{K}^{-1}$) and an isotope effect of 1.3(1).^{19b} The isotope effect for the σ -bond metathesis reaction of $\text{Cp}^*\text{Cp}^*\text{ClHfSiH}_2\text{Ph}$ and PhSiH_3 or PhSiD_3 is 2.7(2), with $\Delta H^\ddagger = 19 \text{ kcal}\cdot\text{mol}^{-1}$ and $\Delta S^\ddagger = -33 \text{ cal}\cdot\text{mol}^{-1}\cdot\text{K}^{-1}$.³⁵ Rare earth-mediated Si–C bond formations provide isotope effects closer to unity.³⁶ For example, Cp^*ScMe and Ph_2SiH_2 or Ph_2SiD_2 react with an isotope effect of 1.15(5) and activation parameters of $\Delta H^\ddagger = 6.6 \text{ kcal}\cdot\text{mol}^{-1}$ and $\Delta S^\ddagger = -43 \text{ cal}\cdot\text{mol}^{-1}\cdot\text{K}^{-1}$. Additionally, the reaction of $\text{To}^M\text{MgNHf-t-Bu}$ and PhMeSiH_2 involving Si–N bond formation occurs with an isotope effect of 1.0(2), $\Delta H^\ddagger = 5.7(2) \text{ kcal}\cdot\text{mol}^{-1}$, and $\Delta S^\ddagger = -46.1(8) \text{ cal}\cdot\text{mol}^{-1}\cdot\text{K}^{-1}$.³⁷ Although a number of variables are not constant between these experiments (including variations in organosilane and metal center as well as various Si–E bond formations including Si–O, Si–N, and Si–C bonds), a rough empirical trend of isotope effect and activation parameters may be noted from the kinetic parameters associated with these reactions. In particular, metathesis reactions involving isovalent metal-mediated group transfer to silicon in which Si–H or Si–D bonds are broken have isotope effects closer to unity in highly ordered transition states ($\Delta S^\ddagger \ll 0$) and small enthalpic activation barriers. While these parameters are not correlated,³⁸ a negative ΔS^\ddagger and a small ΔH^\ddagger for a second-order elementary step together with a primary kinetic isotope effect ~ 1 may indicate an early transition state in which little bond cleavage has occurred. More experiments, as well as theoretical treatments, that probe isotope effects and activation parameters of concerted Si–H bond cleavages/Si–E bond formations are still needed before significant conclusions may be drawn from these observations.

This metathetical pathway is apparently accessible because Zn–O and O–O bond homolysis pathways, which are common for transition-metal alkylperoxides, are not fast in this monomeric zinc system at moderate temperatures. Comproportionation reactions of peroxyzinc and alkylzinc compounds also are inhibited by the tris(oxazolinyl)borate ligand. Once these decomposition pathways are blocked, the reaction chemistry of peroxyzinc compounds provides several intriguing reactions and observations including a nonoxidative peroxy group transfer.

3. CONCLUSION

Aspects of the chemistry of To^MZnOOR **8**–**12** are distinct from transition-metal alkyl peroxides. A particularly interesting comparison is with monomeric $\text{d}^0 \text{Cp}_2\text{ClTiOOR}$ -*t*-Bu, in which $\text{Cp}_2\text{ClTiO}^\bullet$ is easily formed.²⁷ Neither Ti(IV) nor Zn(II) can be further oxidized, yet the apparent homolysis of the O–O bond in the two compounds occurs at very different rates and provides different products. Thus, $\text{Cp}_2\text{ClTiOOR}$ -*t*-Bu produces *tert*-butanol, whereas homolysis reactions of **11** generate Me_2CO . The putative intermediates $\text{To}^M\text{ZnO}^\bullet$ and $\text{Cp}_2\text{ClTiO}^\bullet$ seem to have divergent chemistry that may be associated with empty orbitals on Ti(IV) versus stabilized occupied orbitals on Zn(II). With $3d^n$ transition elements, metal-centered oxidation

may further contribute to the destabilization of alkylperoxides. The tris(pyrazolyl)borato transition-metal alkylperoxides clearly show these effects, and the resulting compounds can oxidize CH bonds.

A second interesting comparison is with the autocatalytic chain reactions of $\text{Tp}^*\text{PtHMe}_2$ and O_2 , where $\text{Tp}^*\text{Me}_2\text{PtOO}^\bullet$ reacts with the thermodynamically stronger Pt–H bond rather than the Pt–Me moiety.³⁹ H-atom abstraction, however, is more plausible than $^\bullet\text{CH}_3$ abstraction, and in this sense the $\text{Tp}^*\text{PtHMe}_2$ oxidation is similar to autocatalytic oxidation of organic compounds (where weaker C–C bonds are less reactive than C–H bonds). While the zinc–carbon BDE's in 1–5 are expected to follow the trend $1 > 2 > 3 > 4 > 5$ and the reaction rates with O_2 follow $5 > 4 \sim 3 \sim 2$ (with 1 not reacting), the unreactive Zn–H bond in 13 is expected to be weaker than the Zn–C bonds. The reaction rate for Zn–Me, Zn–Et, and Zn–CMe₃ follows the expected trend from the BDE's, while Zn–H does not. Thus, unlike the selectivity (i.e., relative rates) of radical chains in autoxidation of hydrocarbyl species that are thought to be governed by C–H BDE's (tertiary > secondary > primary), the radical chains of these reactions are not entirely dominated by cleavage of the weakest Zn–E bond.

4. EXPERIMENTAL SECTION

4.1. General Procedures. All reactions were performed under a dry argon atmosphere using standard Schlenk techniques or under a nitrogen atmosphere in a glovebox, unless otherwise indicated. Benzene, toluene, pentane, diethyl ether, and tetrahydrofuran were dried and deoxygenated using an IT PureSolv system. Benzene-*d*₆ and toluene-*d*₈ were heated to reflux over Na/K alloy and vacuum transferred. Dichloromethane-*d*₂ was vacuum transferred from CaH_2 . To^MZnMe (1),^{19b} To^MZnH (13),^{19a} $\text{H}[\text{To}^M]$,^{20b} $\text{Ti}[\text{To}^M]$,^{20a} and dialkylzincs were synthesized according to literature procedures.⁴⁰ Grignard reagents were purchased from Sigma-Aldrich and transferred to flasks equipped with resealable Teflon valves for storage. *t*-BuOOH (5.5 M in decane), PhMe_2COOH (80% technical grade), and AIBN were purchased from Sigma-Aldrich and stored inside a glovebox freezer at -30°C . Benzyltrimethylsilane was purchased from Gelest. Benzyltrimethylsilane-*d*₁ was synthesized by reduction of benzyltrimethylchlorosilane with LiAlD_4 .

¹H, ¹³C{¹H}, ¹¹B, and ¹⁷O NMR spectra were collected on a Bruker DRX400 or an Avance II 600 spectrometer. ¹⁵N chemical shifts were determined by ¹H–¹⁵N HMBC experiments on a Bruker Avance II 700 spectrometer with a Bruker Z-gradient inverse TXI ¹H/¹³C/¹⁵N 5 mm cryoprobe; ¹⁵N chemical shifts were originally referenced to an external liquid NH_3 standard and recalculated to the CH_3NO_2 chemical shift scale by adding -381.9 ppm. Elemental analyses were performed using a Perkin-Elmer 2400 Series II CHN/S in the Iowa State Chemical Instrumentation Facility.

Caution! High-pressure glass apparatuses, reactions of oxygen and reduced compounds, and peroxide-containing materials must be handled with care. Isolated alkylperoxide compounds 8–12 were tested for possible explosive properties, and they did not ignite with attempted initiation under thermal, physical, or electrical stress. Regardless, only small quantities of alkylperoxides were prepared at a single instance. Thick-walled NMR tubes equipped with J. Young-style resealable Teflon valves (pressured to 100 psi with O_2) were obtained from Wilmad-Labglass and attached to a high-pressure steel manifold through commercial Swagelok fittings.^{8c} The tubes were handled in protective jackets for safety concerns. Due to the potentially pyrophoric and explosive nature of silylalkylperoxides,²⁶ the $\text{BnMe}_2\text{SiOOR}$ (R = Et, *n*-C₃H₇, *i*-C₃H₇ and *t*-Bu) species were not isolated; these compounds were characterized in solution and compared with the corresponding BnMe_2SiOR using ¹H, ¹³C{¹H}, and ²⁹Si NMR spectroscopy.

4.2. Synthetic Methods. **4.2.1. To^MZnEt (2).** Diethylzinc (73.2 mL, 0.0882 g, 0.714 mmol) was added to a solution of HTo^M (0.274 g, 0.714 mmol) in 10 mL of benzene in a dropwise fashion. The solution was stirred for 12 h at room temperature, and then the volatiles were evaporated under reduced pressure. The resulting white solid was washed with pentane to provide analytically pure To^MZnEt (2) as a crystalline white solid (0.304 g, 0.638 mmol, 89.3%). X-ray quality crystals were obtained from a concentrated toluene solution that was allowed to stand at -30°C . ¹H NMR (400 MHz, benzene-*d*₆): δ 0.68 (q, 2 H, ZnCH_2CH_3), 1.02 (s, 18 H, $\text{CNCMe}_2\text{CH}_2\text{O}$), 1.81 (t, 3 H, ZnCH_2CH_3), 3.48 (s, 6 H, $\text{CNCMe}_2\text{CH}_2\text{O}$), 7.35 (t, ³J_{HH} = 4.0 Hz, 1 H, *para*-C₆H₅), 7.53 (t, ³J_{HH} = 4.0 Hz, 2 H, *meta*-C₆H₅), 8.34 (d, ³J_{HH} = 4.0 Hz, 2 H, *ortho*-C₆H₅). ¹³C{¹H} NMR (175 HMz, benzene-*d*₆): δ -2.08 (ZnCH_2CH_3), 15.36 (ZnCH_2CH_3), 28.33 ($\text{CNCMe}_2\text{CH}_2\text{O}$), 65.61 ($\text{CNCMe}_2\text{CH}_2\text{O}$), 80.78 ($\text{CNCMe}_2\text{CH}_2\text{O}$), 126.19 (*para*-C₆H₅), 127.21 (*meta*-C₆H₅), 136.48 (*ortho*-C₆H₅), 142.92 (br, *ipso*-C₆H₅), 190.02 (br, $\text{CNCMe}_2\text{CH}_2\text{O}$). ¹¹B NMR (128 MHz, benzene-*d*₆): δ -17.3 . ¹⁵N{¹H} NMR: δ -155.5 . IR (KBr, cm^{-1}): 2969 (s), 2929 (m), 2896 (m), 1603 (s, ν_{CN}), 1461 (m), 1385 (m), 1366 (m), 1350 (m), 1268 (s), 1193 (s), 1159 (s), 953 (s), 892 (w), 741 (m), 706 (s). Anal. calcd for $\text{C}_{23}\text{H}_{34}\text{BN}_3\text{O}_3\text{Zn}$: C, 57.95; H, 7.19; N, 8.81. Found: C, 57.77; H, 7.10; N, 8.82. Mp 167–170 °C (dec).

Synthesis of 3 is given here as a representative example. Compounds 3–5 and 7 are synthesized following identical procedures. Full experimental details for 4, 5, and 7 are provided in the SI.

4.2.2. $\text{To}^M\text{Zn}(n\text{-C}_3\text{H}_7)$ (3). A suspension of $\text{Zn}(\text{OMe})_2$ (0.174 g, 1.36 mmol) in Et_2O (20 mL) was cooled to 0°C . *n*-C₃H₇MgBr (1.4 mL, 2 M in Et_2O) was added, and the resulting mixture was allowed to warm to room temperature and stir for 1 h. The mixture was filtered to separate the insoluble magnesium salts from $(n\text{-C}_3\text{H}_7)_2\text{Zn}$, and the solution was added to $\text{Ti}[\text{To}^M]$ (0.200 g, 0.341 mmol). Immediately, a black mixture formed. This mixture was stirred for 20 min, the volatile materials were evaporated under reduced pressure, and the residue was extracted with benzene (10 mL). Evaporation of the colorless extracts provided a white solid that was washed with pentane (3×5 mL) and dried under vacuum. Analytically pure $\text{To}^M\text{Zn}(n\text{-C}_3\text{H}_7)$ (0.143 g, 0.291 mmol, 85.3%) was obtained as a white crystalline solid. X-ray quality crystals were grown by slow diffusion of pentane into a concentrated toluene solution standing at -30°C . ¹H NMR (400 MHz, benzene-*d*₆): δ 0.70 (m, 2 H, $\text{ZnCH}_2\text{CH}_2\text{CH}_3$), 1.02 (s, 18 H, $\text{CNCMe}_2\text{CH}_2\text{O}$), 1.46 (t, ³J_{HH} = 7.2 Hz, 3 H, $\text{ZnCH}_2\text{CH}_2\text{CH}_3$), 2.08 (m, 2 H, $\text{ZnCH}_2\text{CH}_2\text{CH}_3$), 3.47 (s, 6 H, $\text{CNCMe}_2\text{CH}_2\text{O}$), 7.37 (t, ³J_{HH} = 6.8 Hz, 1 H, *para*-C₆H₅), 7.56 (t, ³J_{HH} = 7.6 Hz, 2 H, *meta*-C₆H₅), 8.36 (d, ³J_{HH} = 7.2 Hz, 2 H, *ortho*-C₆H₅). ¹³C{¹H} NMR (175 HMz, benzene-*d*₆): δ 10.92 ($\text{ZnCH}_2\text{CH}_2\text{CH}_3$), 23.29 ($\text{ZnCH}_2\text{CH}_2\text{CH}_3$), 24.93 ($\text{ZnCH}_2\text{CH}_2\text{CH}_3$), 28.33 ($\text{CNCMe}_2\text{CH}_2\text{O}$), 65.67 ($\text{CNCMe}_2\text{CH}_2\text{O}$), 80.78 ($\text{CNCMe}_2\text{CH}_2\text{O}$), 126.22 (*para*-C₆H₅), 127.24 (*meta*-C₆H₅), 136.49 (*ortho*-C₆H₅), 146.10 (br, *ipso*-C₆H₅), 190.32 (br, $\text{CNCMe}_2\text{CH}_2\text{O}$). ¹¹B NMR (128 MHz, benzene-*d*₆): δ -17.3 . ¹⁵N{¹H} NMR (71 MHz, benzene-*d*₆): δ -155.8 . IR (KBr, cm^{-1}): 3074 (w), 3045 (w), 2966 (s), 2935 (s), 2825 (m), 1601 (s, ν_{CN}), 1495 (w), 1462 (s), 1432 (w), 1384 (m), 1365 (m), 1354 (m), 1272 (s), 1251 (w), 1195 (s), 1161 (s), 957 (s), 896 (w), 867 (w), 841 (w), 816 (m), 746 (s), 703 (s), 668 (s). Anal. calcd for $\text{C}_{24}\text{H}_{36}\text{BN}_3\text{O}_3\text{Zn}$: C, 58.74; H, 7.39; N, 8.56. Found: C, 58.98; H, 7.59; N, 8.43. Mp 180–184 °C (dec).

4.2.3. To^MZnPh (6). To^MZnCl (0.206 g, 0.426 mmol) and PhLi (0.036 g, 0.430 mmol) were dissolved in THF (12 mL) and stirred for 8 h at ambient temperature. A white solid was obtained by evaporation of the volatile materials, and the residue was extracted with 12 mL of benzene. Evaporation of the benzene, followed by pentane washes (3×5 mL) and drying under vacuum provided crystalline, analytically pure To^MZnPh (0.207 g, 0.394 mmol, 94.5%). X-ray quality single crystals were grown from a concentrated toluene solution of To^MZnPh at -30°C . ¹H NMR (400 MHz, benzene-*d*₆): δ 1.03 (s, 18 H, $\text{CNCMe}_2\text{CH}_2\text{O}$), 3.46 (s, 6 H, $\text{CNCMe}_2\text{CH}_2\text{O}$), 7.38 (m, 1 H, *para*-C₆H₅), 7.38 (m, 1 H, *para*-ZnC₆H₅), 7.51 (vt, *J* = 7.6 Hz, 2 H, *meta*-ZnC₆H₅), 7.58 (vt, *J* = 7.2 Hz, 2 H, *meta*-C₆H₅), 8.09 (d, ³J_{HH} = 7.6 Hz, 2 H, *ortho*-ZnC₆H₅), 8.38 (d, ³J_{HH} = 7.2 Hz, 2 H, *ortho*-C₆H₅). ¹³C{¹H} NMR (175 HMz, benzene-*d*₆): δ 28.40 ($\text{CNCMe}_2\text{CH}_2\text{O}$),

65.86 (CNCMe₂CH₂O), 81.06 (CNCMe₂CH₂O), 126.32 (*para*-C₆H₅), 126.66 (*para*-C₆H₅), 127.28 (*meta*-C₆H₅), 127.95 (*meta*-ZnC₆H₅), 136.49 (*ortho*-C₆H₅), 140.41 (*ortho*-ZnC₆H₅), 142.52 (br, *ipso*-C₆H₅), 154.40 (*ipso*-ZnC₆H₅), 190.52 (br, CNCMe₂CH₂O). ¹¹B NMR (128 MHz, benzene-*d*₆): δ -18.1. ¹⁵N{¹H} NMR: δ -157.4. IR (KBr, cm⁻¹): 3048 (w), 2966 (m), 2928 (w), 2891 (w), 1594 (s, ν_{CN}), 1460 (m), 1389 (m), 1369 (m), 1352 (m), 1275 (s), 1196(s), 1158 (m), 1071 (w), 948 (m), 895 (w), 842 (w), 817 (m), 758 (s), 746 (m), 727 (s), 704 (s). Anal. calcd for C₂₈H₃₆BN₃O₃Zn: C, 61.80; H, 6.53; N, 8.01. Found: C, 61.25; H, 6.30; N, 8.01. Mp: 197–200 °C (dec).

Synthesis of **8** is given here as a representative example. Compounds **8**–**10** are prepared following related procedures. Full experimental details for **9** and **10** are provided in the SI.

4.2.4. To^MZnOOEt (8). A 100 mL resealable Teflon-valved flask was charged with a benzene solution (20 mL) of To^MZnEt (0.450 g, 0.944 mmol). The solution was degassed with freeze–pump–thaw cycles, placed under an atmosphere of O₂, and then sealed. The solution was heated at 60 °C for 12 h and then allowed to cool to room temperature. The volatile materials were removed under reduced pressure. The resulting white residue was washed with pentane (3 × 5 mL) and dried under vacuum yielding analytically pure To^MZnOOEt (**8**; 0.436 g, 0.857 mmol, 90.8%). X-ray quality crystals were grown by allowing pentane to slowly diffuse into a saturated toluene solution of **8** cooled to -30 °C. ¹H NMR (400 MHz, benzene-*d*₆): δ 1.14 (s, 18 H, CNCMe₂CH₂O), 1.40 (t, ³J_{HH} = 6.8 Hz, 3 H, ZnOOCH₂CH₃), 3.48 (s, 6 H, CNCMe₂CH₂O), 4.34 (q, ³J_{HH} = 6.8 Hz, 2 H, ZnOOCH₂CH₃), 7.37 (t, ³J_{HH} = 7.2 Hz, 1 H, *para*-C₆H₅), 7.55 (vt, *J* = 7.6 Hz, 2 H, *meta*-C₆H₅), 8.32 (d, ³J_{HH} = 7.2 Hz, 2 H, *ortho*-C₆H₅). ¹³C{¹H} NMR (175 MHz, benzene-*d*₆): δ 14.85 (ZnOOCH₂CH₃), 28.15 (CNCMe₂CH₂O), 65.67 (CNCMe₂CH₂O), 71.94 (ZnOOCH₂CH₃), 81.19 (CNCMe₂CH₂O), 126.47 (*para*-C₆H₅), 127.35 (*meta*-C₆H₅), 136.36 (*ortho*-C₆H₅), 142.03 (br, *ipso*-C₆H₅), 190.66 (br, CNCMe₂CH₂O). ¹¹B NMR (128 MHz, benzene-*d*₆): δ -17.1. ¹⁵N{¹H} NMR (71 MHz, benzene-*d*₆): δ -159.2. ¹⁷O NMR (81 MHz, benzene-*d*₆): δ 319 (ZnOO(CH₂CH₃)), 169 (ZnOO(CH₂CH₃)). IR (KBr, cm⁻¹): 3083 (w), 3042 (w), 2969 (m), 2929 (w), 2885 (w), 1592 (s, ν_{CN}), 1495 (w), 1462 (s), 1435 (w), 1387 (m), 1368 (m), 1351 (m), 127 (s), 1198 (s), 1164 (s), 963 (s), 898 (w), 819 (w), 744(w). Anal. calcd for C₂₃H₃₄BN₃O₃Zn: C, 54.30; H, 6.73; N, 8.26. Found: C, 54.52; H, 6.74; N, 8.12. Mp: 208–211 °C.

Synthesis of **11** is representative of the procedure for preparation of **12**, which is provided in the SI.

4.2.5. To^MZnOO(*t*-Bu) (11). A solution of To^MZnH (0.550 g, 1.23 mmol) in 12 mL of benzene was treated with *t*-BuOOH (0.23 mL, 5.5 M in decane). The mixture was allowed to stir at room temperature for 1 h. The solvent was then evaporated to obtain a white residue that was washed with pentane (3 × 5 mL) and dried under vacuum affording crystalline, analytically pure **11** (0.549 g, 1.02 mmol, 83.4% yield) as a white solid. X-ray quality single crystals were grown from a concentrated toluene solution of To^MZnOO(*t*-Bu) at -30 °C. ¹H NMR (400 MHz, benzene-*d*₆): δ 1.15 (s, 18 H, CNCMe₂CH₂O), 1.59 (s, 9 H, ZnOOCMe₃), 3.48 (s, 6 H, CNCMe₂CH₂O), 7.37 (t, ³J_{HH} = 7.4 Hz, 1 H, *para*-C₆H₅), 7.55 (vt, *J* = 7.6 Hz, 2 H, *meta*-C₆H₅), 8.32 (d, ³J_{HH} = 7.6 Hz, 2 H, *ortho*-C₆H₅). ¹³C{¹H} NMR (175 MHz, benzene-*d*₆): δ 27.57 (ZnOOCMe₃), 28.16 (CNCMe₂CH₂O), 65.69 (CNCMe₂CH₂O), 77.60 (ZnOOCMe₃), 81.20 (CNCMe₂CH₂O), 126.44 (*para*-C₆H₅), 127.34 (*meta*-C₆H₅), 136.37 (*ortho*-C₆H₅), 142.12 (br, *ipso*-C₆H₅), 190.49 (br, CNCMe₂CH₂O). ¹¹B NMR (128 MHz, benzene-*d*₆): δ -17.1. ¹⁵N{¹H} NMR (71 MHz, benzene-*d*₆): δ -158.8. ¹⁷O NMR (81 MHz, benzene-*d*₆, obtained from To^MZnOOCMe₃ and ¹⁷O₂): δ 284 (ZnOOCMe₃), 204 (ZnOOCMe₃). IR (KBr, cm⁻¹): 3078 (w), 3048 (w), 2967 (m), 2927 (w), 2897 (w), 2870 (w), 1598 (s, ν_{CN}), 1496 (w), 1464 (s), 1433 (w), 1367 (m), 1353 (s), 1278 (s), 1198 (s), 1164 (s), 963 (s), 898 (w), 819 (w), 744 (w). Anal. calcd for C₂₅H₃₈BN₃O₃Zn: C, 55.94; H, 7.14; N, 7.83. Found: C, 55.85; H, 7.38; N, 7.83. Mp: 193–195 °C.

4.2.6. (κ²-To^M)₂Zn (14). To^MZnH (0.250 g, 0.557 mmol) and Ti[To^M] (0.327 g, 0.557 mmol) were dissolved in benzene (15 mL)

and heated to 85 °C for 48 h. A shiny metallic black precipitate appeared during the course of the reaction. A colorless solution was obtained upon filtration. Removal of the volatiles materials from the filtrate gave a white solid that was washed with pentane (3 × 5 mL) and dried under vacuum, affording analytically pure bis(κ²-To^M)Zn (0.417 g, 0.502 mmol, 90.1%) as a white powdery solid. X-ray quality single crystals were grown from a slow pentane diffusion into a concentrated toluene solution of **14** at -30 °C. ¹H NMR (benzene-*d*₆, 400 MHz): δ 0.94 (s, 6 H, CNCMe₂CH₂O), 1.12 (s, 6 H, CNCMe₂CH₂O), 1.23 (s, 6 H, CNCMe₂CH₂O), 1.31 (s, 18 H, CNCMe₂CH₂O), 3.29–3.38 (m, 6 H, ZnNCMe₂CH₂O), 3.51 (d, ³J_{HH} = 8.4 Hz, 2 H, ZnNCMe₂CH₂O), 3.69 (s, 4 H, CNCMe₂CH₂O), 7.25 (t, ³J_{HH} = 7.2 Hz, 2 H, *para*-C₆H₅), 7.44 (t, ³J_{HH} = 7.2 Hz, 4 H, *meta*-C₆H₅), 8.05 (d, ³J_{HH} = 7.2 Hz, 4 H, *ortho*-C₆H₅). ¹³C{¹H} NMR (benzene-*d*₆, 100 MHz): δ 25.80 (ZnNCMe₂CH₂O), 27.84 (ZnNCMe₂CH₂O), 28.64 (ZnNCMe₂CH₂O), 28.66 (ZnNCMe₂CH₂O), 29.57 (CNCMe₂CH₂O), 66.44 (ZnNCMe₂CH₂O), 67.30 (ZnNCMe₂CH₂O), 68.32 (CNCMe₂CH₂O), 77.35 (CNCMe₂CH₂O), 78.67 (ZnNCMe₂CH₂O), 79.18 (ZnNCMe₂CH₂O), 126.15 (*para*-C₆H₅), 127.74 (*meta*-C₆H₅), 134.56 (*ortho*-C₆H₅), 147.40 (*ipso*-C₆H₅), 194 (br, CNCMe₂CH₂O). ¹¹B NMR (benzene-*d*₆, 128 MHz): δ -17.0. ¹⁵N{¹H} NMR (benzene-*d*₆, 71 MHz): δ -120.6 (CNCMe₂CH₂O), -178.9 (CN(Zn)-CMe₂CH₂O). IR (KBr, cm⁻¹): 2966 (s), 2928 (w), 2878 (w), 1604 (m, ν_{CN}), 1560 (s, ν_{CN}), 1490 (w), 1464 (m), 1432 (w), 1369 (m), 1359 (m), 1278 (m), 1250 (m), 1199 (m), 1152 (m), 1002 (s), 969 (s), 892 (w), 848 (w). Anal. calcd for C₄₂H₅₈B₂N₆O₆Zn: C, 60.78; H, 7.04; N, 10.13. Found: C, 60.91; H, 7.38; N, 9.95. Mp 190–195 °C (dec).

4.2.7. (To^MZnOH)₃ (15). A benzene solution of To^MZnOOEt (0.210 g, 0.413 mmol) was photolyzed in a Rayonet chamber at 350 nm for 24 h at ambient temperature. Colorless, X-ray quality crystals were formed during the photolysis. The crystals were isolated by decanting of the supernatant solution. Further grinding and washing with pentane (3 × 5 mL) followed by drying under reduced pressure provided analytically pure To^MZnOH (0.123 g, 0.265 mmol, 64.1%) as a trimeric species. ¹H NMR (400 MHz, methylene chloride-*d*₂, 25 °C): δ 1.26 (s, br, 18 H, CNCMe₂CH₂O), 3.88 (s, br, 6 H, CNCMe₂CH₂O), 7.13 (m, 3 H, *para*- and *meta*-C₆H₅), 7.24 (d, ³J_{HH} = 6.4 Hz, 2 H, *ortho*-C₆H₅). ¹³C{¹H} NMR (175 MHz, methylene chloride-*d*₂, 25 °C): δ 29.59 (CNCMe₂CH₂O), 66.78 (CNCMe₂CH₂O), 79.19 (CNCMe₂CH₂O), 125.92 (*para*-C₆H₅), 127.88 (*meta*-C₆H₅), 133.57 (*ortho*-C₆H₅), 149.42 (br, *ipso*-C₆H₅), 191.09 (br, CNCMe₂CH₂O). ¹¹B NMR (128 MHz, methylene chloride-*d*₂): δ -18.2. ¹⁵N{¹H} NMR (71 MHz, methylene chloride-*d*₂, 25 °C): δ -160.7. IR (KBr, cm⁻¹): 3069 (w), 2969 (m), 2930 (w), 1623 (m, ν_{CN}), 1577 (s, ν_{CN}), 1492 (w), 1462 (m), 1433 (w), 1383 (w), 1367 (m), 1280 (m), 1197 (m), 1160 (m), 1121 (w), 999 (s), 970 (s), 944 (m), 879 (w), 846 (w), 732 (m), 706 (m), 651 (w). Anal. calcd for C₆₃H₉₀B₃N₉O₉Zn₃: C, 54.28; H, 6.51; N, 9.04. Found: C, 54.22; H, 6.30; N, 8.69. Mp 260–263 °C.

4.2.8. General Synthesis of BnMe₂SiOOR (R = Et, *i*-C₃H₇, *t*-Bu). BnMe₂SiH (0.012 g, 0.08 mmol) and To^MZnOOR (0.02 mmol) were allowed to react in benzene-*d*₆ (0.6 mL). Upon completion of the reaction (R = Et, 2 h; R = *i*-C₃H₇, 6 h; R = *t*-Bu, 12 h at 80 °C), the products were identified and characterized by ¹H, ¹³C{¹H}, and ²⁹Si NMR spectroscopy. Equimolar To^MZnH and BnMe₂SiOOR were formed in each reaction. Additionally, the products' spectra were not equivalent with spectra of BnMe₂SiH starting material and BnMe₂SiOR (synthesized below).

4.2.9. General Synthesis of BnMe₂SiOR (R = Et, *i*-C₃H₇, *t*-Bu). BnMe₂SiH (0.014 g, 0.09 mmol) and ROH (equimolar with respect to BnMe₂SiH) were added to To^MZnH (5 mg, 0.01 mmol) dissolved in benzene-*d*₆ (0.6 mL). The resulting solution was heated in a Teflon-valved NMR tube (R = Et, 60 °C, 4 h; R = *i*-C₃H₇, 80 °C, 10 h; R = *t*-Bu, 135 °C, 65 h). Upon completion of the reaction, the products were identified and characterized based on their ¹H, ¹³C{¹H}, and ²⁹Si NMR spectra.

4.2.10. BnMe₂SiOOEt. ¹H NMR (600 MHz, C₆D₆): δ 0.14 (s, 6 H, SiMe₂), 1.04 (t, 3 H, ³J_{HH} = 7.2 Hz, OOCCH₂CH₃), 2.26 (s, 2 H,

PhCH₂), 3.91 (q, 2 H, ³J_{HH} = 7.2 Hz, OCH₂CH₃), 7.06 (m, 3 H, *para*- and *meta*-C₆H₅), 7.15 (m, 2 H, *ortho*-C₆H₅). ¹³C{¹H} NMR (150 MHz, C₆D₆): δ -2.93 (SiMe₂), 13.70 (SiOCH₂CH₃), 25.70 (PhCH₂), 72.76 (SiOCH₂CH₃), 125.14 (*para*-C₆H₅), 129.01 (*meta*-C₆H₅), 129.22 (*ortho*-C₆H₅), 139.12 (*ipso*-C₆H₅). ²⁹Si NMR (120 MHz, C₆D₆): δ 21.63.

4.2.11. BnMe₂SiOEt. ¹H NMR (600 MHz, C₆D₆): δ 0.01 (s, 6 H, SiMe₂), 1.05 (t, 3 H, ³J_{HH} = 7.2 Hz, OCH₂CH₃), 2.06 (s, 2 H, PhCH₂), 3.44 (q, 2 H, ³J_{HH} = 7.2 Hz, OCH₂CH₃), 7.0 (m, 3 H, *para*- and *meta*-C₆H₅), 7.13 (m, 2 H, *ortho*-C₆H₅). ¹³C{¹H} NMR (150 MHz, C₆D₆): δ -1.96 (SiMe₂), 19.09 (SiOCH₂CH₃), 27.34 (PhCH₂), 58.85 (SiOCH₂CH₃), 124.92 (*para*-C₆H₅), 128.94 (*meta*-C₆H₅), 129.08 (*ortho*-C₆H₅), 139.91 (*ipso*-C₆H₅). ²⁹Si NMR (120 MHz, C₆D₆): δ 12.50.

4.2.12. BnMe₂SiO(*i*-C₃H₇). ¹H NMR (600 MHz, C₆D₆): δ 0.15 (s, 6 H, SiMe₂), 1.11 (d, 6 H, ³J_{HH} = 6.0 Hz, OCHMe₂), 2.27 (s, 2 H, PhCH₂), 4.13 (sept, 1 H, ³J_{HH} = 6.0 Hz, OCHMe₂), 7.05 (m, 3 H, *para*- and *meta*-C₆H₅), 7.14 (m, 2 H, *ortho*-C₆H₅). ¹³C{¹H} NMR (150 MHz, C₆D₆): δ -2.79 (SiMe₂), 20.70 (OCHMe₂), 25.80 (PhCH₂), 78.19 (SiOCHMe₂), 125.11 (*para*-C₆H₅), 128.99 (*meta*-C₆H₅), 129.24 (*ortho*-C₆H₅), 139.23 (*ipso*-C₆H₅). ²⁹Si NMR (120 MHz, C₆D₆): δ 21.26.

4.2.13. BnMe₂SiO(*i*-C₃H₇). ¹H NMR (600 MHz, C₆D₆): δ 0.05 (s, 6 H, SiMe₂), 1.07 (d, 6 H, ³J_{HH} = 6.0 Hz, OCHMe₂), 2.11 (s, 2 H, PhCH₂), 3.80 (sept, 1 H, ³J_{HH} = 6.0 Hz, OCHMe₂), 7.03 (m, 3 H, *para*- and *meta*-C₆H₅), 7.16 (m, 2 H, *ortho*-C₆H₅). ¹³C{¹H} NMR (150 MHz, C₆D₆): δ -1.32 (SiMe₂), 26.37 (OCHMe₂), 27.84 (PhCH₂), 65.56 (SiOCHMe₂), 124.90 (*para*-C₆H₅), 128.89 (*meta*-C₆H₅), 129.12 (*ortho*-C₆H₅), 140.01 (*ipso*-C₆H₅). ²⁹Si NMR (120 MHz, C₆D₆): δ 10.38.

4.2.14. BnMe₂SiO(*t*-Bu). ¹H NMR (600 MHz, C₆D₆): δ 0.16 (s, 6 H, SiMe₂), 1.21 (s, 9 H, OCM₃), 2.28 (s, 2 H, PhCH₂), 7.07 (m, 3 H, *para*- and *meta*-C₆H₅), 7.14 (m, 2 H, *ortho*-C₆H₅). ¹³C{¹H} NMR (150 MHz, C₆D₆): δ -2.55 (SiMe₂), 25.80 (PhCH₂), 26.55 (SiOCMe₃), 81.41 (SiOCMe₃), 125.08 (*para*-C₆H₅), 128.80 (*meta*-C₆H₅), 129.19 (*ortho*-C₆H₅), 139.48 (*ipso*-C₆H₅). ²⁹Si NMR (120 MHz, C₆D₆): δ 20.45.

4.2.15. BnMe₂SiO(*t*-Bu). ¹H NMR (600 MHz, C₆D₆): δ 0.10 (s, 6 H, SiMe₂), 1.16 (s, 9 H, OCM₃), 2.14 (s, 2 H, PhCH₂), 7.04 (m, 3 H, *para*- and *meta*-C₆H₅), 7.17 (m, 2 H, *ortho*-C₆H₅). ¹³C{¹H} NMR (150 MHz, C₆D₆): δ 1.09 (SiMe₂), 29.49 (PhCH₂), 32.47 (SiOCMe₃), 65.56 (SiOCMe₃), 125.02 (*para*-C₆H₅), 128.80 (*meta*-C₆H₅), 129.19 (*ortho*-C₆H₅), 140.42 (*ipso*-C₆H₅). ²⁹Si NMR (120 MHz, C₆D₆): δ 4.35.

4.3. Kinetic Experiments of To^MZnEt + O₂. Reactions were monitored with ¹H NMR spectroscopy using a Bruker DRX-400 spectrometer. The concentrations of NMR-active reactants, initiators, and products were determined by comparison of corresponding integrated resonances to the known concentration of the internal standards. The experiments were performed under pseudofirst-order conditions with excess O₂, and the [To^MZnEt] was monitored for at least three half-lives.

4.4. Determination of Rate Dependence on [AIBN]. A benzene-*d*₆ stock solution was prepared to contain known concentrations of cyclooctane (5.2 mM) as an internal standard and To^MZnEt (25 mM). An experiment was initiated by adding a known quantity of AIBN to a measured volume (0.6 mL) of the stock solution; the [AIBN] was then verified by comparison with the internal standard in the integrated ¹H NMR spectrum. The resulting solution was pressurized with O₂ (50 psi) in a high-pressure NMR tube using a high-pressure manifold. The mixture was shaken vigorously and then inserted into a NMR probe that was preheated to 54 °C. The [AIBN] was varied from 5.4 to 31.5 mM. The integrated intensities of To^MZnEt were measured over the reaction time course. For each experiment, the -d[To^MZnEt]/dt followed an exponential decay (Figure S-1, SI) to give *k*_{obs}. The half-order dependence on [AIBN] was obtained by a nonweighted linear least-squares fit of the *k*_{obs} values against [AIBN]^{1/2} (Figure S-2, SI).

4.5. Determination of Rate Dependence on P_{O₂}. A benzene-*d*₆ stock solution containing cyclooctane (9.6 mM), To^MZnEt (33 mM), and AIBN (14.1 mM) was prepared. A known volume of this solution (0.6 mL) was added to a thick-walled J. Young NMR tube. The tube was charged with a measured pressure of O₂ (30–100 psi) using a high-pressure manifold. The tube was shaken vigorously and then placed in a preheated NMR spectrometer probe (54 °C). The integrated intensities of To^MZnEt were measured over the reaction time course. The observed pseudofirst-order rate constants *k*_{obs}, determined from nonlinear least-squares analysis, were identical within error for each O₂ pressure (Figure S-3, SI).

4.6. General Description of ¹H NMR Kinetic Experiments for the Reactions Between To^MZnOOR and P(*p*-C₆H₄Me)₃. A toluene-*d*₈ stock solution containing known concentrations of cyclooctane (9.9 mM) and To^MZnOOR (20 mM) was prepared. A measured quantity of this stock solution (0.6 mL) was placed in a septa-capped NMR tube, and the tube was cooled to -78 °C. Tris(*para*-tolyl)phosphine was dissolved in a minimal amount (50 μL) of toluene-*d*₈, and this solution was added through the septa using a microliter syringe, and the hole was sealed with silicone grease. The sample was placed in a precooled NMR spectrometer probe. Single scan spectra were acquired automatically at preset time intervals. The concentrations of To^MZnOOR, P(*p*-C₆H₄Me)₃, and OP(*p*-C₆H₄Me)₃ were determined by comparison of corresponding integrated resonances to the known concentration of the internal standard. The second-order rate constants (*k*_{obs}) were obtained by a nonweighted linear least-squares fit of the data to the second-order rate law:

$$\ln \frac{[P(p\text{-C}_6\text{H}_4\text{Me})_3]}{[\text{To}^M\text{ZnOOR}]} = \ln \frac{[P(p\text{-C}_6\text{H}_4\text{Me})_3]_0}{[\text{To}^M\text{ZnOOR}]_0} + k_{\text{obs}}\Delta_o t \quad (6)$$

(Figures S-4–8, SI).

4.7. General Description of ¹H NMR Kinetic Experiments for the Reactions Between To^MZnOOR and BnMe₂SiH. A toluene-*d*₈ stock solution containing known concentrations of cyclooctane (15.7 mM) and To^MZnOOEt (20.7 mM) was prepared. A measured quantity of this stock solution (0.6 mL) was placed in a septa-capped NMR tube, and the tube was cooled to -78 °C. BnMe₂SiH (100 mM) was added through the septa using a microliter syringe, and the hole was sealed with silicone grease. The sample was placed in a precooled NMR spectrometer probe. Single scan spectra were acquired automatically at preset time intervals. The concentrations of To^MZnOOEt, BnMe₂SiH, To^MZnH, and BnMe₂SiOOEt were determined by comparison of the corresponding integrated resonances to the known concentration of the internal standard. The second-order rate constants (*k*_{obs}) were obtained by a nonweighted linear least-squares fit of the data to the second-order rate law:

$$\ln \frac{[\text{BnMe}_2\text{SiH}]}{[\text{To}^M\text{ZnOOEt}]} = \ln \frac{[\text{BnMe}_2\text{SiH}]_0}{[\text{To}^M\text{ZnOOEt}]_0} + k_{\text{obs}}\Delta_o t \quad (7)$$

■ ASSOCIATED CONTENT

📄 Supporting Information

Preparations of compounds 4, 5, 7, 9, 10, and 12, plots of kinetic data, and crystallographic data files. This material is available free of charge via the Internet at <http://pubs.acs.org>.

■ AUTHOR INFORMATION

Corresponding Author

sadow@iastate.edu

Notes

The authors declare no competing financial interest.

■ ACKNOWLEDGMENTS

Financial support for this work was provided by the U.S. Department of Energy, Office of Basic Energy Sciences,

Division of Chemical Sciences, Geosciences, and Biosciences through the Ames Laboratory (contract no. DE-AC02-07CH11358). A.D.S. thanks Alfred P. Sloan Foundation for a research fellowship.

REFERENCES

- (1) Porter, M. J.; Skidmore, J. *Chem. Commun.* **2000**, 1215–1225.
- (2) Davies, A. G. *J. Chem. Res.* **2008**, 361–375.
- (3) Klement, I.; Lütjens, H.; Knochel, P. *Tetrahedron* **1997**, *53*, 9135–9144.
- (4) Davies, A. G.; Roberts, B. P. *J. Chem. Soc. B* **1968**, 1074–1078.
- (5) Maury, J.; Feray, L.; Bazin, S.; Clément, J.-L.; Marque, S. R. A.; Siri, D.; Bertrand, M. P. *Chem.—Eur. J.* **2011**, *17*, 1586–1595.
- (6) Cohen, T.; Gibney, H.; Ivanov, R.; Yeh, E. A.-H.; Marek, I.; Curran, D. P. *J. Am. Chem. Soc.* **2007**, *129*, 15405–15409.
- (7) Akindele, T.; Yamada, K.-I.; Tomioka, K. *Acc. Chem. Res.* **2009**, *42*, 345–355.
- (8) (a) Denney, M. C.; Smythe, N. A.; Cetto, K. L.; Kemp, R. A.; Goldberg, K. I. *J. Am. Chem. Soc.* **2006**, *128*, 2508–2509. (b) Konnick, M. M.; Stahl, S. S. *J. Am. Chem. Soc.* **2008**, *130*, 5753–5762. (c) Boisvert, L.; Denney, M. C.; Hanson, S. K.; Goldberg, K. I. *J. Am. Chem. Soc.* **2009**, *131*, 15802–15814. (d) Szajna-Fuller, E.; Bakac, A. *Inorg. Chem.* **2010**, *49*, 781–785. (e) Decharin, N.; Popp, B. V.; Stahl, S. S. *J. Am. Chem. Soc.* **2011**, *133*, 13268–13271.
- (9) (a) Lewiński, J.; Zachara, J.; Gos, P.; Grabska, E.; Kopec, T.; Madura, I.; Marciniak, W.; Prowotorow, I. *Chem.—Eur. J.* **2000**, *6*, 3215–3227. (b) Lewiński, J.; Marciniak, W.; Lipkowski, J.; Justyniak, I. *J. Am. Chem. Soc.* **2003**, *125*, 12698–12699. (c) Lewiński, J.; Śliwiński, W.; Dranka, M.; Justyniak, I.; Lipkowski, J. *Angew. Chem., Int. Ed.* **2006**, *45*, 4826–4829.
- (10) (a) Lewiński, J.; Suwala, K.; Kubisiak, M.; Ochal, Z.; Justyniak, I.; Lipkowski, J. *Angew. Chem., Int. Ed.* **2008**, *47*, 7888–7891. (b) Lewiński, J.; Suwala, K.; Kaczorowski, T.; Galezowski, M.; Gryko, D. T.; Justyniak, I.; Lipkowski, J. *Chem. Commun.* **2009**, 215–217.
- (11) Hollingsworth, N.; Johnson, A. L.; Kingsley, A.; Kociok-Köhn, G.; Molloy, K. C. *Organometallics* **2010**, *29*, 3318–3326.
- (12) (a) Han, R.; Parkin, G. *J. Am. Chem. Soc.* **1990**, *112*, 3662–3663. (b) Han, R.; Parkin, G. *J. Am. Chem. Soc.* **1992**, *114*, 748–757. (c) Bailey, P. J.; Coxall, R. A.; Dick, C. M.; Fabre, S.; Henderson, L. C.; Herber, C.; Liddle, S. T.; Loroño-González, D.; Parkin, A.; Parsons, S. *Chem.—Eur. J.* **2003**, *9*, 4820–4828.
- (13) Lewiński, J.; Ochal, Z.; Bojarski, E.; Tratkiewicz, E.; Justyniak, I.; Lipkowski, J. *Angew. Chem., Int. Ed.* **2003**, *42*, 4643–4646.
- (14) Barron, A. R. *Chem. Soc. Rev.* **1993**, *22*, 93–99.
- (15) Cleaver, W. M.; Barron, A. R. *J. Am. Chem. Soc.* **1989**, *111*, 8967–8969.
- (16) Gorrell, I. B.; Looney, A.; Parkin, G. *J. Chem. Soc., Chem. Commun.* **1990**, 220–222.
- (17) Uhl, W.; Jana, B. *Chem.—Eur. J.* **2008**, *14*, 3067–3071.
- (18) (a) Kitajima, N.; Katayama, T.; Fujisawa, K.; Iwata, Y.; Moro-oka, Y. *J. Am. Chem. Soc.* **1993**, *115*, 7872–7873. (b) Hikichi, S.; Komatsuzaki, H.; Akita, M.; Moro-oka, Y. *J. Am. Chem. Soc.* **1998**, *120*, 4699–4710. (c) Komatsuzaki, H.; Sakamoto, N.; Satoh, M.; Hikichi, S.; Akita, M.; Moro-oka, Y. *Inorg. Chem.* **1998**, *37*, 6554–6555. (d) Hikichi, S.; Okuda, H.; Ohzu, Y.; Akita, M. *Angew. Chem., Int. Ed.* **2009**, *48*, 188–191. (e) Hikichi, S.; Kobayashi, C.; Yoshizawa, M.; Akita, M. *Chem. Asian J.* **2010**, *5*, 2086–2092.
- (19) (a) Mukherjee, D.; Ellern, A.; Sadow, A. D. *J. Am. Chem. Soc.* **2010**, *132*, 7582–7583. (b) Mukherjee, D.; Thompson, R. R.; Ellern, A.; Sadow, A. D. *ACS Catal.* **2011**, *1*, 698–702.
- (20) (a) Ho, H.-A.; Dunne, J. F.; Ellern, A.; Sadow, A. D. *Organometallics* **2010**, *29*, 4105–4114. (b) Dunne, J. F.; Su, J.; Ellern, A.; Sadow, A. D. *Organometallics* **2008**, *27*, 2399–2401.
- (21) Looney, A.; Han, R.; Gorrell, I. B.; Cornebise, M.; Yoon, K.; Parkin, G.; Rheingold, A. L. *Organometallics* **1995**, *14*, 274–288.
- (22) Cordero, B.; Gómez, V.; Platero-Prats, A. E.; Revés, M.; Echeverría, J.; Cremades, E.; Barragán, F.; Alvarez, S. *Dalton Trans* **2008**, 2832–2838.
- (23) Jackson, R. L. *Chem. Phys. Lett.* **1989**, *163*, 315–322.
- (24) (a) Armentrout, P. B.; Beauchamp, J. L. *Acc. Chem. Res.* **1989**, *22*, 315–321. (b) Georgiadis, R.; Armentrout, P. B. *J. Am. Chem. Soc.* **1986**, *108*, 2119–2126.
- (25) van Asselt, A.; Santarsiero, B. D.; Bercaw, J. E. *J. Am. Chem. Soc.* **1986**, *108*, 8291–8293.
- (26) Davies, A. G. *Tetrahedron* **2007**, *63*, 10385–10405.
- (27) (a) DiPasquale, A. G.; Kaminsky, W.; Mayer, J. M. *J. Am. Chem. Soc.* **2002**, *124*, 14534–14535. (b) DiPasquale, A. G.; Hrovat, D. A.; Mayer, J. M. *Organometallics* **2006**, *25*, 915–924.
- (28) Suzuki, H.; Matsuura, S.; Moro-oka, Y.; Ikawa, T. *J. Organomet. Chem.* **1985**, *286*, 247–258.
- (29) Conte, V.; Bortolini, O. In *The Chemistry of Peroxides*; Wiley: Chichester, U.K., 2006; pp 1053–1128.
- (30) (a) Espenson, J. H. *Chemical kinetics and reaction mechanisms*; 2nd ed.; McGraw-Hill: New York, 1995. (b) Taylor, J. R. *An introduction to error analysis: the study of uncertainties in physical measurements*; 2nd ed.; University Science Books: Sausalito, CA, 1997. (c) Morse, P. M.; Spencer, M. D.; Wilson, S. R.; Girolami, G. S. *Organometallics* **1994**, *13*, 1646–1655.
- (31) (a) Tan, H.; Yoshikawa, A.; Gordon, M. S.; Espenson, J. H. *Organometallics* **1999**, *18*, 4753–4757. (b) Adam, W.; Mitchell, C. M.; Saha-Müller, C. R.; Weichold, O. *J. Am. Chem. Soc.* **1999**, *121*, 2097–2103.
- (32) (a) Mimoun, H.; de Saint Laumer, J. Y.; Giannini, L.; Scopelliti, R.; Floriani, C. *J. Am. Chem. Soc.* **1999**, *121*, 6158–6166. (b) Mimoun, H. *J. Org. Chem.* **1999**, *64*, 2582–2589.
- (33) Marciniak, B. *Hydrosilylation: a comprehensive review on recent advances*; Springer: Berlin, Germany, 2009.
- (34) Klement, I.; Knochel, P. *Synlett* **1995**, 1113–1114.
- (35) Woo, H.-G.; Heyn, R. H.; Tilley, T. D. *J. Am. Chem. Soc.* **1992**, *114*, 5698–5707.
- (36) (a) Gountchev, T. I.; Tilley, T. D. *Organometallics* **1999**, *18*, 5661–5667. (b) Sadow, A. D.; Tilley, T. D. *J. Am. Chem. Soc.* **2005**, *127*, 643–656.
- (37) Dunne, J. F.; Neal, S. R.; Engelkemier, J.; Ellern, A.; Sadow, A. D. *J. Am. Chem. Soc.* **2011**, *133*, 16782–16785.
- (38) A reviewer pointed out that reactions with small activation enthalpies can have small or large isotope effects.
- (39) Look, J. L.; Wick, D. D.; Mayer, J. M.; Goldberg, K. I. *Inorg. Chem.* **2009**, *48*, 1356–1369.
- (40) Côté, A.; Charette, A. B. *J. Am. Chem. Soc.* **2008**, *130*, 2771–2773.